



Published in final edited form as:

Int J Radiat Oncol Biol Phys. 2021 June 01; 110(2): 337–347. doi:10.1016/j.ijrobp.2020.12.046.

Microstructural Injury to Corpus Callosum and Intrahemispheric White Matter Tracts Correlate With Attention and Processing Speed Decline After Brain Radiation

Minh-Phuong Huynh-Le, MD, MAS^{*}, Michelle D. Tibbs, MD, MAS^{†,‡}, Roshan Karunamuni, PhD^{†,‡}, Mia Salans, MAS[†], Kathryn R. Tringale, MD, MAS[§], Anthony Yip, MAS[†], Michael Connor, MD[†], Aaron B. Simon, MD, PhD[†], Lucas K. Vitzthum, MD, MAS[†], Anny Reyes, MS^{||}, Anna Christina Macari, MS^{‡,||}, Vitali Moiseenko, PhD[†], Carrie R. McDonald, PhD^{#†,‡,||}, Jona A. Hattangadi-Gluth, MD^{#†,‡}

^{*}Division of Radiation Oncology, George Washington University, Washington, DC

[†]Department of Radiation Medicine and Applied Sciences, University of California San Diego, La Jolla, California

[‡]Center for Multimodal Imaging and Genetics, University of California San Diego, La Jolla, California

[§]Department of Radiation Oncology, Memorial Sloan Kettering Cancer Center, New York, New York

^{||}Department of Psychiatry, University of California San Diego, La Jolla, California

[#] These authors contributed equally to this work.

Abstract

Purpose: The corpus callosum (CC) and intrahemispheric white matter tracts (IHWM) subserve critical aspects of attention and processing speed. We analyzed imaging biomarkers of microstructural injury within these regions and association with attention and processing speed performance before and after radiation therapy in primary brain tumor patients.

Methods and Materials: In a prospective clinical trial, 44 primary brain tumor patients underwent cognitive testing and magnetic resonance imaging/diffusion-weighted imaging at baseline (pre-radiation therapy) and 3-, 6-, and 12-months post-radiation therapy. CC (subregions, total) and IHWM tracts (left/right without CC, total) were autosegmented; tumor, tumor bed, and edema were censored. Biomarkers included volume changes (cm³), mean diffusivity ([MD]; higher values indicate white matter injury), fractional anisotropy ([FA]; lower values indicate white matter injury). Reliable-change indices measured changes in attention (Wechsler Adult Intelligence Scale [WAIS-IV] digits-forward; Delis-Kaplan Executive Function System Trail Making [D-KEFS-TM] visual-scanning), and processing speed (WAIS-IV coding; D-KEFS-TM number-sequencing, letter-sequencing), accounting for practice effects. Linear mixed-effects

Corresponding author: Jona A. Hattangadi-Gluth, MD; jhattangadi@ucsd.edu.

Research data are stored in an institutional repository and will be shared upon request to the corresponding author.

Supplementary material for this article can be found at <https://doi.org/10.1016/j.ijrobp.2020.12.046>.

models evaluated associations between mean radiation dose and biomarkers (volume, MD, FA) and imaging biomarkers and neurocognitive performance. Statistics were corrected for multiple comparisons.

Results: Processing speed declined at 6 months following radiation therapy (number sequencing, letter sequencing; $P < .04$). Seizures and antiepileptic drug therapy were associated with lower visual-scanning attention reliable-change indices at 6 months ($P = .039$). Higher radiation dose correlated with smaller midanterior CC volume ($P = .023$); lower FA in posterior CC, anterior CC, and total CC (all $P < .03$); and higher MD in anterior CC ($P = .012$). Smaller midanterior CC and left IHWM volume correlated with worse processing speed (coding, letter-sequencing, number-sequencing; all $P < .03$). Higher FA in right, left, and total IHWM correlated with better coding scores (all $P < .01$). Lower FA in total IHWM ($P = .009$) was associated with worse visual-scanning attention scores. Higher FA in midposterior CC ($P = .029$) correlated with better digits-forward attention scores.

Conclusions: The CC demonstrated radiation dose-dependent atrophy and WM injury. Microstructural injury within the CC and IHWM was associated with attention and processing speed decline after radiation therapy. These areas represent possible avoidance regions for preservation of attention and processing speed.

Introduction

Attention and processing speed are core cognitive domains implicated in radiation therapy (RT)-associated neurocognitive decline, with clear effects on quality of life, activities of daily living, and interpersonal relationships.¹⁻³ Attention (ie, the ability to focus, release, and transfer stimuli) is linked to other cognitive functions, motor ability, and social behavior,³⁻⁵ whereas processing speed (ie, how quickly one can complete a mental task and understand and react to inputs^{6,7}) may influence higher-level intelligence and cognition.⁸ Deficits may manifest as the inability to follow sequential cooking directions in a recipe, identify needed ingredients in a store, or focus on work.⁹ Unfortunately, RT-mediated attention and processing speed decline remains underevaluated,¹⁰⁻¹⁴ even as neurocognitive function is now being studied as the primary endpoint in modern interventional studies.^{10,15}

Attention and processing speed are subserved by a diffuse brain white matter (WM) network, including the corpus callosum (CC) and WM association and projection fibers. These association and projection fibers are collectively referred to as the intrahemispheric WM tracts (IHWM). The CC is the major interhemispheric WM commissure connecting the 2 cerebral hemispheres, with more than 200 to 300 million fibers transferring information and connecting homotopic and heterotopic cortical regions in humans.¹⁶ CC injury influences processing speed, visuospatial processing, and attention.¹⁷⁻²² In pediatrics, CC atrophy after brain RT is correlated with decline in attention and working memory.²³ The CC genu and body may be particularly susceptible to radiation-mediated injury in children.²⁴ Others have reported RT-induced injury to 2 major CC subregions (genu and splenium) in adults.²⁵ Attention and processing speed also rely on a broad network of intrahemispheric WM tracts, as opposed to being localized cognitive functions specific to one or a few WM tracts regions.^{5,7,18,19,26-29} WM injury may negatively influence attention and processing speed.^{5,18,19,30}

Diffusion tensor imaging and volumetric brain magnetic resonance imaging (MRI) allow quantitative, noninvasive measurements of microstructural brain tissue in vivo, including measurements of WM integrity^{31–33} and volume changes.^{34,35} Recent diffusion tensor imaging studies have identified biomarkers of RT-associated WM microstructural injury,^{31–33} with changes in these biomarkers—including fractional anisotropy (FA) and mean diffusivity (MD)—associated with cognitive decline after RT.^{33,36} Attention and processing speed have been explored in children receiving RT given the potentially devastating effects of RT on brain neural development,^{6,23,24} but longitudinal data in adults with brain tumors are lacking. Here, we present the first comprehensive, prospective analysis of longitudinal attention and processing speed functioning in adult patients with primary brain tumors before and after RT, and the underlying microstructural IHWM tract and CC injury that may contribute.

Materials and Methods

Patients

This prospective, observational clinical trial was approved by the institutional review board. Written, informed consent was obtained from all patients.

A total of 59 adult patients with primary brain tumors requiring fractionated, partial brain RT using either photons or protons between 2014 and 2018 were eligible for enrollment. Inclusion criteria were Karnofsky performance status ≥ 70 , estimated life expectancy ≥ 1 year, and ability to undergo neurocognitive testing in English. Exclusion criteria included prior brain RT. Patients underwent diffusion and volumetric high-resolution MRI and a battery of neurocognitive tests pre-RT, and at 3-, 6-, and 12-months post-RT. Patients were evaluated clinically and radio-graphically for signs of tumor progression and recurrence. Participants with evidence of tumor progression or recurrence during the study period were removed from the study, as per protocol. These patients would continue with standard of care follow-up and radiographic imaging. A total of 44 patients had at least 2 timepoints of imaging and neurocognitive testing available and were included in the analyses (Fig. E1).

MRI acquisition, processing, and registration

MRI scans were acquired using a previously described, institutional standardized protocol^{36–38} on a 3.0T 750 GE system (GE Health Care, Milwaukee, WI) with an 8-channel coil. Sequences obtained included: 3-dimensional volumetric T1-weighted, T2-weighted fluid-attenuated inversion recovery, and diffusion-weighted imaging (DWI). Additional image acquisition details are available in the supplementary material.

The T1/T2/DWI MRI sequences were coregistered in a common space. Images were processed using algorithms written in MATLAB (MathWorks, Natick, MA) to correct for spatial and geometric distortions from gradient nonlinearities, susceptibility, and eddy currents.^{36–38} Images were meticulously inspected for registration or segmentation errors. We manually created a censoring mask, drawn slice-by-slice, comprised of the tumor, surgical bed, edema (T2 fluid-attenuated inversion recovery hyperintensity), and other radiographic abnormalities separately for each patient at each timepoint. All voxels in the

censoring mask were eliminated from analysis to avoid confounding from tumor and edema effects.

The CC was autosegmented using FreeSurfer 5.3.0 (available at <http://surfer.nmr.mgh.harvard.edu>), which automatically parcellates the volumetric T1-weighted pre-contrast MRI data into regions of interest (ROI).³⁹ ROIs included total CC and CC subdivided into 5 subregions: anterior (corresponds to the rostrum), midanterior (genu), central (truncus/body), midposterior (anterior splenium), and posterior (posterior splenium) (Fig. 1).⁴⁰ Different CC subdivisions are implicated in the control of distinct cognitive functions²² and may be selectively affected by RT.^{24,25}

Brain total IHWM tracts, including all long-range association and projection fiber tracts, were autosegmented using an automated white matter atlas-based tractography system developed at our institution (AtlasTrack⁴¹) using the DWI sequences. Total IHWM was subdivided into right-sided IHWM without CC (right IHWM) and left-sided IHWM without CC (left IHWM) to explore the possible effects of laterality (Fig. 1). The volume (in cc) of each WM ROI at each timepoint was determined for evaluation of possible RT-associated volume changes.

Diffusion metrics (MD and FA) for a given ROI at a particular timepoint were determined by averaging over the ROI voxels at that timepoint. MD is an average of 3 eigenvalues representing the mobility of water molecules, with higher values indicating WM injury.⁴² FA is an index ranging from 0 to 1 and is a biomarker representing the directionality of water diffusion and WM microstructural instability, with lower values indicating WM injury.⁴²

ROI dose determination

MRI data were rigidly registered to the patients' computed tomography simulation images acquired during RT planning and subsequently postprocessed. Images were carefully reviewed for registration errors. The resulting transformation matrix was used to resample the RT dose distribution into the T1-weighted MRI volume space as previously described.^{36–38} Mean dose to each ROI was calculated.

Neurocognitive testing

Formal assessments of attention and processing speed were obtained at each timepoint. Three tests evaluated processing speed: Delis-Kaplan Executive Function System Trail Making (D-KEFS-TM)⁴³ Number Sequencing (TM-NS), D-KEFS-TM Letter Sequencing (TM-LS), and Weschler Adult Intelligence Scale (WAIS-IV)⁴⁴ Coding. The TM-NS and TM-LS tests have participants rapidly connect numbers and letters, respectively, in sequential order.⁴³ The Coding subtest evaluates the ability to quickly pair visual stimuli.⁴⁴

Two tests measured attention. Visual attention was assessed using the D-KEFS-TM Visual Scanning (TM-VS) test, which evaluates the ability to focus, release, and transfer visuospatial attention.⁴³ In the TM-VS test, participants are asked to quickly find and cross out all the number 3s, which are presented among other letters and numbers. Auditory attention was evaluated via the WAIS-IV⁴⁴ Digit Span Digits Forward (DF) test. The DF test asks participants to verbally repeat a sequence of numbers in the same order back to an

examiner after being read that sequence, measuring simple attention, efficiency, and mental capacity.⁴⁴

The WAIS-IV and D-KEFS-TM are well-validated tests with alternate forms (accounting for repeated testing), minimizing practice effects. Importantly, the raw score output varies by assessment. The D-KEFS-TM subtests (TM-NS, TM-LS, and TM-VS) all have raw scores representing the time in seconds that the patient required to complete the task,⁴³ with greater scores signifying worse performance. Alternatively, in the WAIS-IV Coding and DF subtests, greater scores represent a higher output of correct responses and better performance.⁴⁴ Raw scores were converted to standardized or T-scores, with adjustments for age and sex, when appropriate.⁴⁵

Reliable change indices (RCI), quantifications of whether the change in neurocognitive scores per test is significant for individual patients, were calculated between baseline and 6-month scores using the standardized neurocognitive scores (T-scores).⁴⁶ Baseline to 6-month change was analyzed as this timepoint approximates the shift from subacute to long-term, irreversible RT-associated damage.² RCIs were adjusted for practice effects (RCI-PE), accounting for repeated testing.⁴⁷

Statistical analyses

Sample *t* tests ($H_0 = 0$) were used to determine significant group decline in RCI-PEs. Associations between RCI-PEs and patient or tumor characteristics (age, sex, race/ethnicity, highest education level, tumor location, glioma vs benign tumor, surgery type, RT type [proton vs photon], size of the RT planning target volume, chemotherapy receipt during study period, seizures during study period, and antiepileptic drug [AED] treatment) were assessed via Pearson correlations, independent samples *t* tests, and 1-way analysis of variance, as appropriate ($\alpha = 0.05$).

RT dose as predictor of injury biomarkers

We evaluated the mean dose to each ROI as a predictor of the outcomes of volume, FA, and MD for each ROI over time via linear mixed-effects (LME; R *lme4* package) models with subject-specific random intercepts. Time was included as a main effect. We controlled for the percentage of the ROI censored as a main effect for analyses with volume as the outcome due to potential for confounding as a result of manual censoring over time. We corrected for multiple comparisons using the false discovery rate.⁴⁸

Injury biomarkers as predictors of attention and processing speed performance

We assessed the effects of imaging biomarkers (volume, MD, FA) and time as predictors of attention and processing speed performance (outcome) with LME models, again with subject-specific random intercepts and time as a main effect. Raw neurocognitive scores were used for these LME models.^{37,38} As described earlier, we controlled for percentage of ROI censored in all models where volume was a predictor variable and corrected for multiple comparisons using the false discovery rate.⁴⁸

Results

Patients

Demographics of the cohort ($n = 44$) are presented in Table 1. The median age was 47 years (range, 20–75 y). Most patients were men and non-Hispanic white, and most (59%) had glioma. Half of the patients received chemotherapy and approximately half had seizures or received AED therapy. No patients in the cohort experienced tumor progression or recurrence during the 1-year study period (Fig. E1).

Baseline to 6-month post-RT attention and processing speed RCI-PEs are shown in Table 2. Significant group decline was seen in the TM-NS (mean RCI-PE, -0.39 ; $P = .03$) and TM-LS (mean RCI-PE, -0.42 ; $P = .006$) processing speed tests. No significant group decline was seen for the Coding, DF, or TM-VS tests.

Seizures and AEDs were significantly associated with lower TM-VS attention RCI-PEs at 6 months ($F = 4.65$; $P = .039$ for both). All patients with seizures in the TM-VS subanalysis received AEDs. Patients with seizures showed decline in TM-VS attention (mean RCI-PE, -0.59 ; standard deviation, 0.77), compared with those without seizures (mean RCI-PE, 0.07; standard deviation, 0.97). No significant associations were seen between other clinical variables (including glioma vs benign histology, chemotherapy receipt, or planning target volume size) and RCI-PE scores for the other 4 cognitive tests.

Relationship between RT dose and injury biomarkers

Table 1E shows the mean doses received to each ROI. The relationship between mean RT dose received by each ROI and imaging biomarkers are shown in Table 3. After controlling for time and correction for multiple comparisons, higher mean dose was associated with smaller volumes within the midanterior CC ($\beta = -0.00140$; $P = .023$). Higher mean dose correlated with lower FA in the posterior CC ($\beta = -0.01635$; $P < .001$), anterior CC ($\beta = -0.1046$; $P = .026$), and total CC ($\beta = -0.0751$; $P = .029$). Higher mean dose was also associated with higher MD in the anterior CC ($\beta = 0.00185$; $P = .012$). Mean dose was not significantly associated with imaging biomarkers within IHWM tracts (left, right, and total).

Injury biomarkers as predictors of processing speed performance

Raw processing speed scores as predicted by volume change, FA, and MD of the CC and IHWM tracts ROIs are shown in Table 4. After correction for multiple comparisons, smaller volume of the left IHWM tracts was associated with poorer processing speed (TM-NS [$\beta = -0.454$; $P = .025$], TM-LS [$\beta = -0.510$; $P = .024$], and Coding [$\beta = 0.636$; $P = .004$]). Smaller midanterior CC volume was associated with worse Coding ($\beta = 37.800$; $P = .011$) scores. Larger volume within the total IHWM ($\beta = 0.156$; $P = .046$) was associated with better Coding performance.

Higher FA values in the right IHWM ($\beta = 2.202$; $P = .008$), left IHWM ($\beta = 2.154$; $P = .007$), and the total IHWM tracts ($\beta = 2.924$; $P = .0004$) were all associated with better Coding performance after corrections for multiple comparisons. Higher FA in the midposterior CC trended toward significance for association with better Coding performance ($\beta = 0.360$; P

= .042). No significant associations were seen between MD and processing speed performance.

Injury biomarkers as predictors of attention performance

Raw attention scores as predicted by volume change, FA, and MD of the CC and IHWM tracts ROIs are shown in Table 5. After correction for multiple comparisons, lower FA values within the total IHWM tracts ($\beta = -1.411$; $P = .009$) were associated with poorer TM-VS performance. Higher FA in the midposterior CC ($\beta = 0.078$; $P = .029$) was significantly associated with better DF scores. Lower FA in the left IHWM ($\beta = -1.162$; $P = .040$) and right IHWM ($\beta = -1.162$; $P = .035$) trended toward significant associations with worse TM-VS scores. There were no significant relationships between volume or MD and attention performance.

Discussion

Attention and processing speed deficits are important components within the constellation of cognitive impairments that emerge after brain RT.^{2,3} We present the first longitudinal, prospective study to evaluate RT-mediated injury to the CC and IHWM tracts in adults with primary brain tumors as predictors of attention and processing speed decline. We found correlations between RT dose and imaging biomarkers of CC injury. Furthermore, we demonstrated associations between imaging biomarkers of injury in the CC and IHWM, and poorer attention and processing speed performance after RT. There was significant subacute decline in processing speed performance, providing further evidence that RT may negatively affect this essential cognitive function. Overall, we affirm the importance of WM pathways, specifically the CC and IHWM tracts, in attention and processing speed control after brain RT.^{7,16–20}

We found RT-dose dependent injury to the CC and its subregions: smaller volume, lower FA, and higher MD. This is consistent with previous work showing that the CC is particularly vulnerable to dose-dependent injury.^{24,25,31} Here, no one subregion appeared more susceptible: injury was seen in the total, anterior, midanterior, and posterior CC. Dose-dependent microstructural injury of the CC has implications for attention and processing speed performance. Interestingly, similar dose-dependent changes were not seen in the IHWM tracts evaluated (left, right, and total IHWM). This is likely because these are large intrahemispheric WM structures and analyzing mean RT dose as a predictor led to an overall washout of dose effect. Others have found dose-dependent WM changes using voxel- or tract-based morphometry to parcellate structures into smaller subunits.^{31,33}

With respect to processing speed, there was significant group decline at 6 months in the TM-NS and TM-LS tests. This is important as D-KEFS-TM performance can be predictive of whether adults with neurologic diseases like Parkinson's are able to complete their activities of daily living.⁹ Post-RT deterioration in the ability to rapidly, sequentially connect numbers and letters may be detrimental to the daily functioning of patients with primary brain tumors, many of whom may already demonstrate cognitive deficits before the initiation of RT.⁴⁹ Interestingly, we did not find associations between age and processing speed decline (RCI-PE) at 6 months; prior literature suggests a slowing of cognitive processing speed capacity,

mediated by microstructural WM injury, as adults age.^{18,19,50} Our findings are likely due to the relatively young age of our cohort (median, 47 y overall, 45 y for patients with gliomas). Indeed, trial candidacy included good life expectancy and excellent pre-RT performance status. These high functioning patients with long life expectancy are the ones in whom preservation of neurocognitive functioning is essential, regardless of tumor histology.

Volume atrophy in CC subregions and IHWM tracts was associated with poorer processing speed performance. Additionally, higher FA within IHWM tracts and CC subregions correlated with better processing speed performance. These results are concordant with data on cognitive impairment from noncancer populations, suggesting that more intricate measures of processing speed (ie, reaction time) are heavily regulated by CC size and IHWM tract integrity.^{18,19,51} Similar evidence exists for both adult and pediatric patients with brain tumors.^{23,24,30} The CC is postulated to have micro- and macrostructural fibers working in dual excitatory-inhibitory connections, facilitating rapid interhemispheric information transfer.^{16,21} RT-induced CC injury can therefore dramatically influence processing speed. Also, loss of bilateral WM tract integrity can affect processing speed.^{26,29} It is thus unsurprising that longitudinal IHWM injury and CC atrophy were associated with worse processing speed performance in our cohort.

Regarding attention, there was no subacute group decline in visual or auditory attention. However, seizures and AED therapy were associated with TM-VS visual attention decline. This is consistent with literature demonstrating TM-VS deficits in patients with temporal lobe epilepsy.⁵² Deficits in TM-VS have also been identified in patients with depression and mood disturbances.⁵³ Attention is intricately linked to neurocognitive plasticity³⁻⁵ and other cognitive functions, including learning, memory, and executive functioning. Ultimately, attention is a “gateway” to overall cognition: if one cannot attend, most everything downstream of that is disrupted. Thus, post-RT visual attention impediments in certain patients (eg, those with seizures) may significantly affect other key parts of their overall cognitive functioning.

Longitudinal injury to IHWM tracts was associated with poorer visual attention performance. Attention is mediated by more distributed WM networks (as opposed to being subserved by a single brain structure or localized network), which rely heavily on cortical-subcortical connections.^{2,27,28} WM damage is linked to attention deficits in children after RT.⁵⁴ Therefore, WM microstructural injury—reflected by lower FA within total IHWM in this cohort—is expected to negatively affect attention. As for auditory attention, we found that higher FA of the midposterior CC was associated with better DF performance. The DF test evaluates simple auditory attention: storing information for short amounts of time. Damage to CC subregions may influence DF performance in individuals with chronic low back pain.⁵⁵ The microstructural organization of the CC, in facilitating interhemispheric transfer of information, is crucial for proper attention function.²¹ Overall, CC and IHWM tract injury appear critical to visual and auditory attention function after brain RT.

These findings beg the question of how to mitigate attention and processing speed decline in patients with brain tumors receiving RT. Much work focuses on the hippocampus and its role in memory¹⁰; the prospective NRG-CC001 trial evaluating hippocampal-sparing whole brain

RT (WBRT) revealed better memory preservation with hippocampal avoidance in patients with brain metastases.¹⁰ Attention and processing speed are equally important to overall cognitive functioning, but deficits may be less obvious in standard clinical settings where formal neurocognitive testing is not routinely available. Perhaps limiting dose to the CC (or its subregions) can lessen decline. CC dose-avoidance efforts could readily be incorporated: the CC is easily identified by radiation oncologists without need for advanced neuroimaging. CC-sparing WBRT is already being studied for patients with brain metastases in an ongoing clinical trial ([NCT03223922](#)) evaluating the preservation of neurocognitive functioning after genu-sparing WBRT. However, CC-sparing RT may be challenging to achieve for gliomas. The same interhemispheric connections that make the CC a critical cognitive highway also allow for glial spread of both low- and high-grade gliomas to the contralateral hemispheres. Indeed, the full extent of low-grade gliomas can manifest as T2 hyperintensities. To account for this, we meticulously excluded all tumor involvement and voxels with T2 hyperintensity from analysis. Further investigation is needed to ensure adequate tumor coverage while avoiding CC overtreatment in efforts to improve attention and processing speed.

Irrespective of the CC, there are diffuse WM tracts that influence attention and processing speed function.^{5,7,18,19,26,29} We found biomarkers of IHWM atrophy and loss of IHWM tract integrity (while excluding the CC) to be associated with neurocognitive changes. The bilateral IHWM was affected by RT, again demonstrating the widespread nature of attention and processing speed control throughout the brain. Patients may benefit from RT techniques designed to minimize dose to uninvolved or contralateral brain IHWM. Possible strategies include noncoplanar volumetric arc techniques⁵⁶ or leveraging proton RT to spare normal tissue distal to tumor. The NRG-BN005 phase 2 trial is actively studying cognitive preservation (primary endpoint) via proton RT for low- or intermediate-grade World Health Organization grade 2 and 3 gliomas. Regardless of technique, sparing uninvolved brain tissue during RT planning may help alleviate the devastating symptoms and sequelae of attention and processing speed decline.

This hypothesis-generating, exploratory study has some limitations. The sample size is relatively small, although this prospective trial cohort is similar or larger in size to other seminal studies investigating neurocognitive changes after brain RT.^{25,30,33} Because these are patients with primary brain tumors, we deliberately censored tumor, surgical changes, T2 hyperintensity, and edema to measure true incidental RT-induced injury to the CC and IHWM tracts. There remains, however, the possibility of microscopic tumor infiltration beyond the visible tumor and surgical bed, particularly for patients with high-grade gliomas. Our cohort was heterogeneous, although tumor type (glioma vs benign) was not associated with attention or processing speed performance. Chemotherapy⁵⁷ or disease progression and recurrence can also affect neurocognition. However, here, receipt of chemotherapy was not correlated with attention and processing speed decline and no patients experienced tumor progression. Therefore, inclusion of diverse patients allows for meaningful cognitive assessments relevant to most primary brain tumor patients, increasing the generalizability of our findings. Altogether, we have demonstrated radiation dose-dependent injury in the CC, in addition to associations between CC and IHWM microstructural injury and attention/processing speed decline. Future endeavors into attention and processing speed preservation after brain RT are critical to improving patient functioning and overall quality of life.

Conclusion

We found selective RT dose-dependent atrophy and WM injury to CC subregions. Additionally, we demonstrated associations between RT-mediated microstructural injury to the CC and IHWM tracts, and attention and processing speed decline in patients with primary brain tumors. The CC and IHWM therefore represent possible RT avoidance structures for preservation of attention and processing speed function post-RT. Further study of cognitive-sparing brain RT is needed to mitigate attention and processing speed decline after RT.

Supplementary Material

Refer to Web version on PubMed Central for supplementary material.

Acknowledgments

This work was supported by the National Institutes of Health (1TL1TR001444 to KRT; 1TL1TR001443 to MDT, MS, and AY; UL1TR001442 of CTSA funding in support of UC San Diego Clinical and Translational Research Institute, and 1KL2TR001444, UL1TR000100, R01 CA238783-01 to JAH-G), National Cancer Institute and UC San Diego Moores Cancer Center (P30 CA02310029 to JAH-G), and American Cancer Society (ACS-IRG 70-002 to CRM). The content is solely the responsibility of the authors and does not necessarily represent the official views of any of the funding agencies, who had no direct role in designing, conducting, or reporting the study.

Disclosures: JAH-G reports grant funding from Varian Medical Systems, unrelated to the present study. CRM has received research funding from GE Health Care, unrelated to the current study. There are no financial or other relationships that might lead to a perceived conflict of interest.

References

1. Meyers CA, Brown PD. Role and relevance of neurocognitive assessment in clinical trials of patients with CNS tumors. *J Clin Oncol* 2006;24:1305–1309. [PubMed: 16525186]
2. Makale MT, McDonald CR, Hattangadi-Gluth JA, Kesari S. Mechanisms of radiotherapy-associated cognitive disability in patients with brain tumours. *Nat Rev Neurol* 2016;13:52–64. [PubMed: 27982041]
3. Saad S, Wang TJC. Neurocognitive deficits after radiation therapy for brain malignancies. *Am J Clin Oncol* 2015;38:634–640. [PubMed: 25503433]
4. Yang HL, Chu H, Kao CC, et al. Construction and evaluation of multidomain attention training to improve alertness attention, sustained attention, and visual-spatial attention in older adults with mild cognitive impairment: a randomized controlled trial. *Int J Geriatr Psychiatry* 2020;35:537–546. [PubMed: 31994767]
5. Subramaniam K, Gill J, Fisher M, Mukherjee P, Nagarajan S, Vinogradov S. White matter microstructure predicts cognitive training-induced improvements in attention and executive functioning in schizophrenia. *Schizophr Res* 2018;193:276–283. [PubMed: 28689758]
6. Jacobson LA, Mahone EM, Yeates KO, Ris MD. Processing speed in children treated for brain tumors: effects of radiation therapy and age. *Child Neuropsychol* 2019;25:217–231. [PubMed: 29621934]
7. Turken AU, Whitfield-Gabrieli S, Bammer R, Baldo JV, Dronkers NF, Gabrieli JDE. Cognitive processing speed and the structure of white matter pathways: convergent evidence from normal variation and lesion studies. *Neuroimage* 2008;42:1032–1044. [PubMed: 18602840]
8. Schatz J, Kramer JH, Ablin A, Matthay KK. Processing speed, working memory, and IQ: A developmental model of cognitive deficits following cranial radiation therapy. *Neuropsychology* 2000;14:189–200. [PubMed: 10791859]

9. Higginson CI, Lanni K, Sigvardt KA, Disbrow EA. The contribution of trail making to the prediction of performance-based instrumental activities of daily living in Parkinson's disease without dementia. *J Clin Exp Neuropsychol* 2013;35:530–539. [PubMed: 23663116]
10. Brown PD, Gondi V, Pugh S, et al. Hippocampal avoidance during whole-brain radiotherapy plus memantine for patients with brain metastases: phase III trial NRG oncology CC001. *J Clin Oncol* 2020; 38:1019–1029. [PubMed: 32058845]
11. Chang EL, Wefel JS, Hess KR, et al. Neurocognition in patients with brain metastases treated with radiosurgery or radiosurgery plus whole-brain irradiation: a randomised controlled trial. *Lancet Oncol* 2009;10: 1037–1044. [PubMed: 19801201]
12. Brown PD, Jaeckle K, Ballman KV, et al. Effect of radiosurgery alone vs radiosurgery with whole brain radiation therapy on cognitive function in patients with 1 to 3 brain metastases a randomized clinical trial. *JAMA* 2016;316:401–409. [PubMed: 27458945]
13. Brown PD, Ballman KV, Cerhan JH, et al. Postoperative stereotactic radiosurgery compared with whole brain radiotherapy for resected metastatic brain disease (NCCTG N107C/CEC3): a multicentre, randomised, controlled, phase 3 trial. *Lancet Oncol* 2017;18:1049–1060. [PubMed: 28687377]
14. Brown PD, Pugh S, Laack NN, et al. Memantine for the prevention of cognitive dysfunction in patients receiving whole-brain radiotherapy: a randomized, double-blind, placebo-controlled trial. *Neuro Oncol* 2013;15:1429–1437. [PubMed: 23956241]
15. Lin NU, Wefel JS, Lee EQ, et al. Challenges relating to solid tumour brain metastases in clinical trials, part 2: neurocognitive, neurological, and quality-of-life outcomes. A report from the RANO group. *Lancet Oncol* 2013;14:407–416.
16. Aboitiz F, Scheibel AB, Fisher RS, Zaidel E. Fiber composition of the human corpus callosum. *Brain Res* 1992;598:143–153. [PubMed: 1486477]
17. Paul LK. Developmental malformation of the corpus callosum: a review of typical callosal development and examples of developmental disorders with callosal involvement. *J Neurodev Disord* 2011;3:3–27. [PubMed: 21484594]
18. Salami A, Eriksson J, Nilsson LG, Nyberg L. Age-related white matter microstructural differences partly mediate age-related decline in processing speed but not cognition. *Biochim Biophys Acta* 2012;1822: 408–415. [PubMed: 21930202]
19. Kerchner GA, Racine CA, Hale S, et al. Cognitive processing speed in older adults: relationship with white matter integrity. *PLoS One* 2012; 7:e50425. [PubMed: 23185621]
20. Maheshwari M, Klein AP, Ulmer JL. White matter: functional anatomy of key tracts. In: *Functional Neuroradiology: Principles and Clinical Applications*. New York, NY: Springer; 2012.
21. Chechlacz M, Humphreys GW, Sotiropoulos SN, Kennard C, Cazzoli D. Structural organization of the corpus callosum predicts attentional shifts after continuous theta burst stimulation. *J Neurosci* 2015;35:15353–15368. [PubMed: 26586822]
22. Jokinen H, Ryberg C, Kalska H, et al. Corpus callosum atrophy is associated with mental slowing and executive deficits in subjects with age-related white matter hyperintensities: the LADIS Study. *J Neurol Neurosurg Psychiatry* 2007;78:491–496. [PubMed: 17028118]
23. Rashid A, Ram AN, Kates WR, et al. A prospective study of corpus callosum regional volumes and neurocognitive outcomes following cranial radiation for pediatric brain tumors. *Child's Nerv Syst* 2017;33: 965–972. [PubMed: 28455540]
24. Redmond KJ, Hildreth M, Sair HI, et al. Association of neuronal injury in the genu and body of corpus callosum after cranial irradiation in children with impaired cognitive control: a prospective study. *Int J Radiat Oncol Biol Phys* 2018;101:1234–1242. [PubMed: 29908790]
25. Nagesh V, Tsien CI, Chenevert TL, et al. Radiation-induced changes in normal-appearing white matter in patients with cerebral tumors: a diffusion tensor imaging study. *Int J Radiat Oncol Biol Phys* 2008;70: 1002–1010. [PubMed: 18313524]
26. Kuznetsova KA, Maniega SM, Ritchie SJ, et al. Brain white matter structure and information processing speed in healthy older age. *Brain Struct Funct* 2016;221:3223–3235. [PubMed: 26254904]
27. Fuster JM. Frontal lobe and cognitive development. *J Neurocytol* 2002;31:373–385. [PubMed: 12815254]

28. Stuss DT. Frontal lobes and attention: Processes and networks, fractionation and integration. *J Int Neuropsychol Soc* 2006;12:261–271. [PubMed: 16573859]
29. Penke L, Maniega SM, Murray C, et al. A general factor of brain white matter integrity predicts information processing speed in healthy older people. *J Neurosci* 2010;30:7569–7574. [PubMed: 20519531]
30. Aukema EJ, Caan MWA, Oudhuis N, et al. White matter fractional anisotropy correlates with speed of processing and motor speed in young childhood cancer survivors. *Int J Radiat Oncol Biol Phys* 2009; 74:837–843. [PubMed: 19117694]
31. Connor M, Karunamuni R, McDonald C, et al. Regional susceptibility to dose-dependent white matter damage after brain radiotherapy. *Radiother Oncol* 2017;123:209–217. [PubMed: 28460824]
32. Connor M, Karunamuni R, McDonald C, et al. Dose-dependent white matter damage after brain radiotherapy. *Radiother Oncol* 2016;121: 209–216. [PubMed: 27776747]
33. Chapman CH, Zhu T, Nazem-Zadeh M, et al. Diffusion tensor imaging predicts cognitive function change following partial brain radiotherapy for low-grade and benign tumors. *Radiother Oncol* 2016;120:234–240. [PubMed: 27418525]
34. Seibert TM, Karunamuni R, Bartsch H, et al. Radiation dose—dependent hippocampal atrophy detected with longitudinal volumetric magnetic resonance imaging. *Int J Radiat Oncol Biol Phys* 2017;97:263–269. [PubMed: 28068234]
35. Huynh-Le M-P, Karunamuni R, Moiseenko V, et al. Dose-dependent atrophy of the amygdala after radiotherapy. *Radiother Oncol* 2019; 136:44–49. [PubMed: 31015128]
36. Tringale KR, Nguyen T, Bahrami N, et al. Identifying early diffusion imaging biomarkers of regional white matter injury as indicators of executive function decline following brain radiotherapy: A prospective clinical trial in primary brain tumor patients. *Radiother Oncol* 2019; 132:27–33. [PubMed: 30825966]
37. Tringale KR, Nguyen TT, Karunamuni R, et al. Quantitative imaging biomarkers of damage to critical memory regions are associated with post–radiation therapy memory performance in brain tumor patients. *Int J Radiat Oncol Biol Phys* 2019;105:773–783. [PubMed: 31408667]
38. Tibbs MD, Huynh-Le MP, Karunamuni R, et al. Microstructural injury to left-sided perisylvian white matter predicts language decline after brain radiation therapy. *Int J Radiat Oncol Biol Phys* 2020;108:1218–1228. [PubMed: 32712255]
39. Fischl B, Salat DH, Busa E, et al. Whole brain segmentation: automated labeling of neuroanatomical structures in the human brain. *Neuron* 2002;33:341–355. [PubMed: 11832223]
40. Collinson SL, Gan SC, Woon PS, et al. Corpus callosum morphology in first-episode and chronic schizophrenia: combined magnetic resonance and diffusion tensor imaging study of Chinese Singaporean patients. *Br J Psychiatry* 2014;204:55–60. [PubMed: 24202961]
41. Hagler DJ, Ahmadi ME, Kuperman J, et al. Automated white-matter tractography using a probabilistic diffusion tensor atlas: application to temporal lobe epilepsy. *Hum Brain Mapp* 2009;30: 1535–1547. [PubMed: 18671230]
42. Alexander AL, Lee JE, Lazar M, Field AS. Diffusion tensor imaging of the brain. *Neurotherapeutics* 2007;4:316–329. [PubMed: 17599699]
43. Delis DC, Kaplan EKJ. Delis-Kaplan Executive Function System (DKEFS). San Antonio, TX: The Psychological Corporation; 2001.
44. Wechsler D Manual for the Wechsler Adult Intelligence Scale. 4th ed. New York, NY: The Psychological Corporation; 2008.
45. Tibbs MD, Huynh-Le MP, Reyes A, et al. Longitudinal analysis of depression and anxiety symptoms as independent predictors of neurocognitive function in primary brain tumor patients. *Int J Radiat Oncol Biol Phys* 2020;108:1229–1239. [PubMed: 32634542]
46. Jacobson NS, Truax P. Clinical significance: a statistical approach to defining meaningful change in psychotherapy research. *J Consult Clin Psychol* 1991;59:12–19. [PubMed: 2002127]
47. Chelune GJ, Naugle RI, Lüders H, Sedlak J, et al. Individual change after epilepsy surgery: Practice effects and base-rate information. *Neuropsychology* 1993;7:41–52.
48. Benjamini Y, Hochberg Y. Controlling the false discovery rate: a practical and powerful approach to multiple testing. *J R Stat Soc* 1995; 57:289–300.

49. Karunamuni R, Tringale KR, Burkeen J, et al. Multi-domain neurocognitive classification of primary brain tumor patients prior to radiotherapy on a prospective clinical trial. *J Neurooncol* 2020;146: 131–138. [PubMed: 31760596]
50. MacPherson SE, Cox SR, Dickie DA, et al. Processing speed and the relationship between Trail Making Test-B performance, cortical thinning and white matter microstructure in older adults. *Cortex* 2017; 95:92–103. [PubMed: 28865241]
51. Anstey KJ, Mack HA, Christensen H, et al. Corpus callosum size, reaction time speed and variability in mild cognitive disorders and in a normative sample. *Neuropsychologia* 2007;45: 1911–1920. [PubMed: 17240409]
52. Galioto R, Tremont G, Blum AS, LaFrance WC, Crook CL, Davis JD. Depressive symptoms contribute to executive deficits in temporal lobe epilepsy. *J Neuropsychiatry Clin Neurosci* 2017;29:135–141. [PubMed: 27707196]
53. Peterson RK, Noggle CA, Thompson JC, Barisa MT, Maulucci A. Differential patterns of performance on the DKEFS in the presence of pediatric mood disturbances. *Neuropsychol Trends* 2017;22: 47–55.
54. Mulhern RK, White HA, Glass JO, et al. Attentional functioning and white matter integrity among survivors of malignant brain tumors of childhood. *J Int Neuropsychol Soc* 2004;10:180–189. [PubMed: 15012838]
55. Buckalew N, Haut MW, Morrow L, Weiner D. Chronic pain is associated with brain volume loss in older adults: preliminary evidence. *Pain Med* 2008;9:240–248. [PubMed: 18298708]
56. Papp D, Bortfeld T, Unkelbach J. A modular approach to intensity-modulated arc therapy optimization with noncoplanar trajectories. *Phys Med Biol* 2015;60:5179–5198. [PubMed: 26083759]
57. Wefel JS, Saleeba AK, Buzdar AU, Meyers CA. Acute and late onset cognitive dysfunction associated with chemotherapy in women with breast cancer. *Cancer* 2010;116:3348–3356. [PubMed: 20564075]

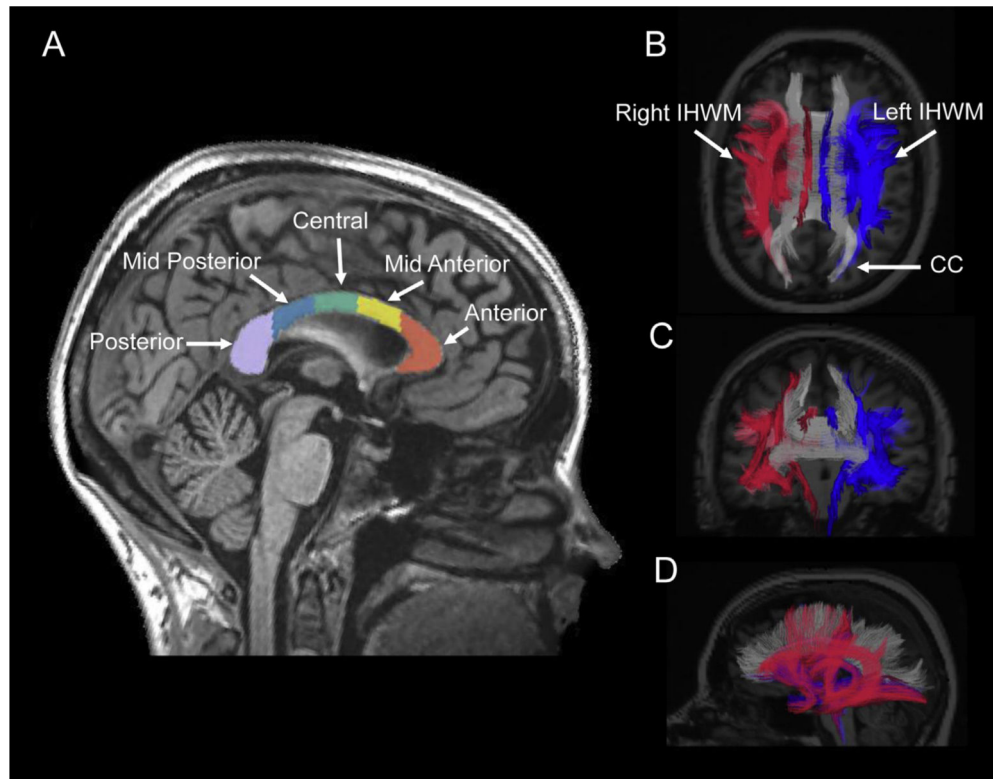


Fig. 1. Overlay of autosegmentation of total corpus callosum (CC) and intrahemispheric white matter (IHWM) tracts on magnetic resonance images taken from a representative patient in the cohort. (A) Total CC and its subregions: anterior, midanterior, central, midposterior, and posterior, derived from FreeSurfer. (B) Axial, (C) coronal, and (D) sagittal images of left and right IHWM tracts generated from diffusion weighted imaging using AtlasTract. Right IHWM is shown in red, left IHWM is blue, and CC is gray.

Table 1

Demographics and clinical characteristics of the 44 study participants

Characteristic	Patients, n (%)
Median age (range), y	47 (20–75)
Sex	
Male	25 (57)
Female	19 (43)
Race/ethnicity	
Non-Hispanic white	34 (77)
Hispanic	5 (11)
Black	1 (2)
Other*	4 (10)
Highest education achieved, median (range), y	15.5 years (10–20)
High school	8 (18)
College	22 (50)
Graduate school	14 (32)
Tumor type	
Glioma, WHO grade 3–4 [†]	18 (41)
Glioma, WHO grade 1–2 [‡]	8 (18)
Meningioma	9 (20)
Pituitary adenoma	4 (9)
Schwannoma	2 (5)
Craniopharyngioma	2 (5)
Low-grade chondrosarcoma	1 (2)
Tumor side	
Left	21 (48)
Right	19 (43)
Central	4 (9)
Tumor region	
Frontal	14 (32)
Temporal	10 (23)
Suprasellar	8 (18)
Parietal	3 (7)
Base of skull	3 (7)
Cerebellar	3 (7)
Cavernous sinus	2 (5)
Sphenoid wing	1 (2)
Radiation therapy type	
IMRT/VMAT	31 (70)
Proton	13 (30)
Radiation therapy dose and fractionation	

Characteristic	Patients, n (%)
54 Gy/30 fractions	14 (32)
59.4 Gy/33 fractions	14 (32)
50.4 Gy/28 fractions	7 (16)
60 Gy/30 fractions	7 (16)
70 Gy/35 fractions [§]	1 (2)
Radiation planning target volume, median (interquartile range), cc	155.8 (48.3–228.2)
Baseline preradiation therapy Karnofsky performance status	
100	14 (32)
90	27 (61)
80	3 (7)
Surgery type	
Gross total resection	9 (20)
Subtotal resection	27 (61)
Biopsy	3 (7)
None	5 (12)
Chemotherapy during study period	22 (50)
Concurrent/adjuvant temozolomide	14
Concurrent/adjuvant temozolomide, and other ^{//}	5
Adjuvant procarbazine, lomustine, and vincristine	3
History of seizures during study period	20 (45)
Antiepileptic drug therapy during study period	23 (52)

Abbreviations: IMRT = intensity-modulated radiation therapy; VMAT = volumetric modulated arc therapy; WHO = World Health Organization.

* Other race/ethnicity included Asian (n = 2) and Middle Eastern (n = 2).

[†] WHO grade 3–4 gliomas included: grade 3 anaplastic astrocytoma (IDH1 mutated, MGMT methylated [n = 7]; IDH1 wildtype, MGMT methylated [n = 1]); grade 3 anaplastic oligodendroglioma, IDH1 mutated, 1p/19q codeleted (n = 2); grade 4 glioblastoma multiforme (IDH1 wildtype, MGMT methylated [n = 4]; IDH1 wildtype, MGMT unmethylated [n = 3]; glioblastoma not otherwise specified [n = 1]).

[‡] WHO grade 1–2 gliomas included: grade 1 pilocytic astrocytoma (n = 1); grade 2 ependymoma (n = 1); grade 2 oligodendroglioma, IDH1-mutated, 1p/19q codeleted (n = 3); grade 2 diffuse astrocytoma (IDH1 wildtype, MGMT methylated [n = 1]; IDH1 wildtype, MGMT unmethylated [n = 1], IDH1 mutated, MGMT methylated [n = 1]).

[§] Patient treated for low-grade chondrosarcoma.

^{//} Other chemotherapy included: adjuvant lomustine (n = 1), poly (ADP-ribose) polymerase-inhibitor clinical trial (n = 1), and vaccine clinical trial (n = 3).

Table 2

Baseline to 6-month RCI-PEs for the attention and processing speed tests included in this study

Domain	Neurocognitive Test	Mean RCI-PE (SD)	P Value
Processing speed	D-KEFS-TM Number sequencing (n = 34)	-0.39 (1.01)	.03*
	D-KEFS-TM Letter sequencing (n = 34)	-0.42 (0.83)	.006*
	WAIS-IV Coding (n = 32)	-0.41 (1.40)	.10
Attention	WAIS-IV Digits forward (n = 35)	0.12 (1.24)	.58
	D-KEFS-TM ^a Visual scanning (n = 34)	-0.24 (0.93)	.14

Abbreviations: D-KEFS-TM = Delis-Kaplan Executive Function System Trail Making; RCI-PE = reliable change indices with practice effects; SD = standard deviation; WAIS-IV = Weschler Adult Intelligence Scale IV.

* Indicates a statistically significant *P* value.

Table 3

Mean radiation dose as predictors of biomarker injury: linear-mixed-effects analysis of mean RT dose (Gy) as a predictor of volume, FA, and MD of each brain ROI, while controlling for time

Outcome	Brain Region	Estimate (β) [*]	Standard Error	P Value
Volume [†]	Total CC	-0.00760	-0.00402	.068
	Posterior CC	-0.00151	0.00127	.237
	Mid-Posterior CC	-0.00061	0.00052	.240
	Central CC	-0.00083	0.0005	.105
	Mid-Anterior CC	-0.00140	0.0006	.023
	Anterior CC	-0.00201	0.00134	.139
	Total IHWM	-0.0805	0.222	.718
	Right IHWM	-0.0854	0.068	.212
	Left IHWM	-0.0185	0.0615	.764
FA	Total CC	-0.0751	0.0334	.029[‡]
	Posterior CC	-0.1635	0.0346	<.001[‡]
	Mid-Posterior CC	-0.0375	0.0339	.273
	Central CC	-0.0164	0.0316	.605
	Mid-Anterior CC	-0.0045	0.0335	.893
	Anterior CC	-0.1046	0.0457	.026[‡]
	Total IHWM	-0.0274	0.0236	.250
	Right IHWM	-0.0179	0.0195	.362
	Left IHWM	-0.0173	0.0185	.352
MD	Total CC	0.000746	0.000553	.180
	Posterior CC	0.000722	0.000458	.120
	Mid-Posterior CC	0.000464	0.000447	.302
	Central CC	0.000597	0.000425	.163
	Mid-Anterior CC	0.000606	0.000544	.267
	Anterior CC	0.00185	0.000716	.012[‡]
	Total IHWM	0.000173	0.000536	.747
	Right IHWM	0.000244	0.000452	.589
	Left IHWM	0.000107	0.000432	.805

Abbreviations: CC = corpus callosum; FA = fractional anisotropy; IHWM = intrahemispheric white matter tracts; MD = mean diffusivity; ROI = region of interest; RT = radiation therapy.

Significant results ($P < .05$) are shown in bold.

^{*} β estimate units are Gy/(mo*cm³) for volume, Gy/mo for FA, and Gy/(mo* μ m²/ms) for MD.

[†] Volume models control for percentage of ROI censored.

[‡] Results that remained significant after corrections for multiple comparisons.

Table 4

Linear mixed-effects model results of imaging biomarkers of injury (volume, FA, and MD) as predictors of processing speed raw scores.

Region	Biomarker	Processing Speed								
		D-KEFS-TM Number Sequencing			D-KEFS-TM Letter Sequencing			WAIS Coding		
		Estimate (β)*	Standard Error	P Value	Estimate (β)	Standard Error	P value	Estimate (β)	Standard Error	P Value
Total CC	Volume	1.110	2.340	.640	-6.870	2.580	.791	3.780	2.280	.099
	FA	-0.293	0.241	.227	-0.086	0.255	.737	0.438	0.233	.062
	MD	12.123	10.838	.264	-8.587	11.017	.427	-5.377	10.266	.601
Posterior CC	Volume	4.210	6.500	.518	-0.183	7.690	.981	6.590	7.360	.372
	FA	-0.168	0.149	.262	-0.121	0.157	.442	0.219	0.149	.142
	MD	6.137	11.163	.583	-9.679	11.358	.395	-4.231	10.894	.698
Mid-Posterior CC	Volume	6.420	12.400	.606	-2.690	13.100	.837	16.700	12.000	.169
	FA	-0.029	0.191	.881	-0.060	0.201	.765	0.360	0.175	.042
	MD	6.544	10.231	.523	-4.977	10.332	.630	-8.604	9.382	.360
Central CC	Volume	5.010	13.500	.721	-11.400	14.300	.427	18.400	12.800	.155
	FA	-0.202	0.210	.337	0.054	0.221	.808	0.265	0.197	.180
	MD	11.803	10.599	.268	-11.271	10.686	.293	-2.816	9.784	.774
Mid-Anterior CC	Volume	-14.200	13.500	.300	-24.400	14.900	.109	37.800	14.600	.011 [†]
	FA	-0.172	0.200	.393	0.075	0.210	.722	0.135	0.167	.420
	MD	8.906	9.129	.330	-8.541	9.248	.357	-3.591	8.517	.674
Anterior CC	Volume	3.780	7.300	.612	0.224	8.440	.979	8.770	8.120	.281
	FA	-0.103	0.183	.578	-0.012	0.197	.950	0.327	0.188	.086
	MD	10.781	8.100	.187	-3.174	8.266	.701	-4.481	7.511	.551
Total IHWM	Volume	-0.101	0.068	.141	-0.113	0.077	.146	0.156	0.077	.046 [†]
	FA	-0.777	0.670	.249	-0.173	0.807	.831	2.924	0.806	.0004 [†]
	MD	13.327	14.136	.347	-14.346	14.214	.314	-7.713	13.396	.565
Right IHWM	Volume	-0.026	0.203	.899	-0.111	0.237	.641	0.354	0.245	.155
	FA	-0.080	0.682	.907	0.221	0.802	.783	2.202	0.811	.008 [†]
	MD	11.737	14.355	.414	-15.419	14.438	.287	-7.456	13.572	.583

Region	Biomarker	Processing Speed											
		D-KEFS-TM Number Sequencing				D-KEFS-TM Letter Sequencing				WAIS Coding			
		Estimate (β)*	Standard Error	P Value	Estimate (β)	Standard Error	P value	Estimate (β)	Standard Error	P Value	Estimate (β)	Standard Error	P Value
Left IHWM	Volume	-0.454	0.201	.025 [†]	-0.510	0.218	.024 [†]	0.636	0.218	.004 [†]	0.636	0.218	.004 [†]
	FA	-1.052	0.675	.125	-0.242	0.793	.768	2.154	0.781	.007 [†]	2.154	0.781	.007 [†]
	MD	14.151	14.010	.314	-15.401	14.006	.273	-6.603	13.324	.620	-6.603	13.324	.620

Abbreviations: CC = corpus callosum; D-KEFS-TM = Delis-Kaplan Executive Function System Trail Making; FA = fractional anisotropy; IHWM = intrahemispheric white matter tracts; MD = mean diffusivity; ROI = region of interest; RT = radiation therapy; WAIS-IV = Wechsler Adult Intelligence Scale IV.

Note: Processing speed was assessed via the D-KEFS-TM Number Sequencing and Letter Sequencing tests and the WAIS-IV Coding test. Models for each ROI and imaging parameter were created and analyzed independently. All volume models control for percentage of ROI censored. Significant results ($P < .05$) are shown in bold.

* β estimate units are points/($\text{mo}^3 \cdot \text{cm}^3$) for volume; points/mo for FA, and points/($\text{mo}^2 \cdot \mu\text{m}^2/\text{ms}$) for MD.

[†] Results that remained significant after corrections for multiple comparisons.

Table 5

Linear mixed-effects model results of imaging biomarkers of injury (volume, FA, and MD) as predictors of attention raw scores.

Region	Biomarker	Attention					
		WAIS Digits Forward			D-KEFS-TM Visual Scanning		
		Estimate (β)*	Standard Error	P Value	Estimate (β)	Standard Error	P Value
Total CC	Volume	-0.027	0.419	.949	-2.101	-1.890	.268
	FA	0.042	0.046	.367	-0.021	0.196	.918
	MD	-1.192	2.690	.662	1.584	8.836	.858
Posterior CC	Volume	-0.343	1.230	.786	-3.330	5.570	.552
	FA	0.009	0.029	.768	-0.028	0.121	.819
	MD	-1.382	2.715	.611	3.724	9.052	.683
Mid-Posterior CC	Volume	0.896	2.330	.701	-5.880	10.100	.562
	FA	0.078	0.035	.029 [†]	-0.013	0.155	.936
	MD	-2.446	2.413	.328	3.516	8.302	.673
Central CC	Volume	0.377	2.470	.879	-9.860	10.900	.375
	FA	0.045	0.038	.241	-0.048	0.171	.783
	MD	-2.522	2.461	.311	4.891	8.644	.572
Mid-Anterior CC	Volume	-1.230	2.520	.627	-13.200	10.900	.229
	FA	0.035	0.034	.308	-0.012	0.163	.943
	MD	-2.454	2.093	.243	4.198	7.430	.574
Anterior CC	Volume	0.179	1.340	.900	-11.300	5.860	.062
	FA	0.011	0.035	.766	-0.013	0.147	.928
	MD	0.753	1.744	.670	-2.117	6.509	.745
Total IHWM	Volume	-0.002	0.013	.906	0.018	0.055	.748
	FA	0.085	0.127	.505	-1.411	0.510	.009 [†]
	MD	-1.657	3.732	.660	12.190	11.473	.292
Right IHWM	Volume	-0.024	0.039	.532	0.158	0.163	.335
	FA	-0.012	0.131	.927	-1.162	0.529	.035
	MD	-1.033	3.835	.789	14.078	11.629	.230
Left IHWM	Volume	0.026	0.038	.512	-0.052	0.170	.758

		Attention					
		WAIS Digits Forward			D-KEFS-TM Visual Scanning		
Region	Biomarker	Estimate (β)*	Standard Error	P Value	Estimate (β)	Standard Error	P Value
	FA	0.085	0.129	.525	-1.162	0.528	.040
	MD	-1.851	3.706	.623	9.424	11.375	.412

Abbreviations: CC = corpus callosum; D-KEFS-TM = Delis-Kaplan Executive Function System Trail Making; FA = fractional anisotropy; IHWM = intrahemispheric white matter tracts; MD = mean diffusivity; ROI = region of interest; RT = radiation therapy; WAIS-IV = Wechsler Adult Intelligence Scale IV.

Note: Attention was measured via the WAIS Digits Forward and the D-KEFS Trail Making Visual Scanning tests. Models for each region of interest (ROI) and imaging parameter were created and analyzed independently. All volume models control for percentage of ROI censored. Significant results ($P < .05$) are shown in bold.

* β estimate units are points/($\text{mo}^3 \cdot \text{cm}^3$) for volume; points/mo for FA, and points/($\text{mo}^2 \cdot \mu\text{m}^2/\text{ms}$) for MD.

[†] Results that remained significant after corrections for multiple comparisons.